PRAMANA
— journal of
physics

Vol. 41, No. 3,
September 1993
pp. 257–269

Laser produced plasma: A pumping source for cadmium photo-ionization laser

REKHA TAMBAY and RAJ K THAREJA
Department of Physics and Centre for Laser Technology, Indian Institute of Technology, Kanpur 208 016 India

MS received 1 September 1992; revised 20 July 1993

Abstract. We report laser oscillations in Cd II on $4d^9 5s^2\ ^2D_{5/2} - 4d^{10} 5p^2 P_{3/2}$ transition at 441.6 nm using laser produced tungsten plasma as a pumping source. Mach Zehnder interferometer is used to measure electron density. Design and working of the crossed heat pipe used in the studies is discussed.

Keywords. Heat pipe; plasma; laser; photo-ionization; black body

PACS Nos **42.55; 52.50**

1. Introduction

The first proposal for observing population inversion in VUV and X-ray region was due to Duguay and Rentzepis [1]. The early experiments used X-ray filters to eliminate unwanted spectral components from the pumping source. Harris *et al* [2] suggested using a laser produced plasma (LPP) to excite the vapor or the gas. The scheme essentially reduces the separation between the source and the excitation region [3]. Silfvast *et al* [4], using the similar configuration, were the first to demonstrate photo-ionization laser. Since then there have been many reports [5, 6] on the observtion of population inversion using X-ray pumping. Lundberg *et al* [7] observed inversion densities in Zn^+ at 747.8 nm by photo ionizing inner *d* shell electron with a broad band soft X-ray source. Photo-ionization laser in cesium vapor in the range 665–800 nm using a single and multispot plasma has also been reported [8–10]. A 116 nm H_2 laser pumped by a travelling wave photo-ionization electron source has been reported by Benerofe *et al* [11]. Sher *et al* [12] have studied the saturation of Xe III 109 nm laser using travelling wave laser produced plasma excitation. Similar arrangement [13] has been used to study Auger pumped lasers in xenon (108.9 nm) and krypton (90.7 nm). The lasers are pumped by photo-ionization of inner shell electrons followed by Auger decay into excited states. Recently a magnesium photo-ionization laser at 24.7 nm has been proposed [14].

It is known that by focussing the laser radiation to a small area on to a solid target it is possible to create high temperature and high density plasma. Besides laser energy and wavelength the plasma characteristics depend on the physical properties of the target material. The plasma emission is primarily due to free-bound and line radiation. However, for a high *Z* solid target, the continuum emission dominates [15] over line radiation. The broadband emission in a thin layer close to the target surface can be approximated to a black body with temperature as that of the plasma. For lower intensities ($\sim 10^{10}$ W/cm^2) the temperature [16] of the plasma is given by,

$$T \approx (I\lambda^2)^{4/9}$$

while for higher intensities ($\sim 10^{13}$ W/cm^2) the temperature scales as,

$$T \approx 0.6(I\lambda^2)^{2/3}.$$

Studies on LPP of different target materials, in the intensity range 10^{11}–10^{12} W/cm^2 have shown that for high Z elements the peak of the emission spectrum is shifted towards shorter wavelength [17]. Thus by choosing the target material we can match the emission spectrum with that of the photo-ionization cross section. The conversion efficiency of laser energy into photon flux in the soft X-ray region up to 50% has been reported [18]. The laser produced plasmas of a high atomic number transition element such as tungsten, tantalum etc. have been used as black body sources.

In the present work we have studied cadmium metal vapor plasma in a crossed heat pipe. The studies were done with and without a background LPP. A Nd:YAG (DCR-4G, Spectra Physics) laser and its harmonics delivering 1 J energy in 8.0 ns (FWHM) at fundamental was used for plasma production. Laser oscillations were observed in Cd II at 441.6 nm using tungsten plasma as a pumping source. Electron density was measured using a Mach Zehnder interferometer in which heat pipe formed one arm of the interferometer. The present report is organized as follows: In § 2 experimental set up and various diagnostics developed for this work are described. Section 3 contains the studies on metal vapor plasma in a heat pipe. In § 4 cadmium photo-ionization laser on $4d^9 5s^2\,{}^2D_{5/2} - 4d^{10} 5p\,{}^2P_{3/2}$ transition at 441.6 nm is described. In § 5 we discuss various aspects of the present work.

2. Experimental techniques

Heat pipe is a well known device for producing homogeneous metallic vapors. The early experiments for generation of homogeneous metallic vapors used furnaces of different types; hot cathode diode, atomic beam devices, burner systems or other similar instruments. However, to get homogeneous temperature and density distribution, sophisticated radiation shields and heat baffles were used with most of these devices [19, 20]. Another difficulty was that of the windows. Since at high temperature many vaporized species are highly reactive, vapors were kept away from windows by means of traps. Even for nonreactive vapors, the temperature of the windows was kept higher in order to prevent vapor condensation on the windows. Either of the techniques introduces uncertainties in determining the number density of particles because of poorly defined boundary layers. This uncertainty can be reduced by using a 'heat pipe' [21]. The device has been successfully used in resonance fluorescence experiments on alkali molecules [22], harmonic generation in metal vapor gas mixture [23] and also for metal vapor lasers. However, the dynamics in a heat pipe oven cannot be worked out in a simple way, the optimum working conditions have been determined in an empirical way. It is observed that if the central part of the heat pipe is overheated the conditions are changed [24, 25].

Figure 1 shows a crossed heat pipe used for our studies. The crossed heat pipe was made using a stainless steel pipe of 2.5 cm diameter and of 2–3 mm wall thickness. The length of each arm of the pipe was 16 cm. An annular stainless steel plate with

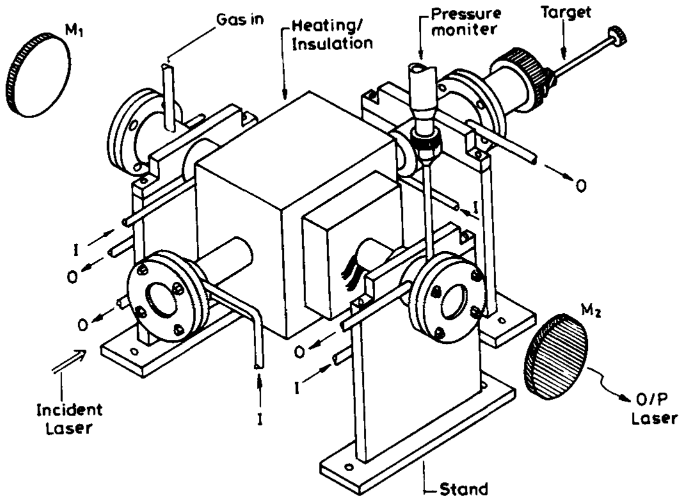

Figure 1. Design of crossed heat pipe.

O-ring groove was welded to each end of the pipe. Quartz windows were pressed on to the pipe by O-rings contained in the annular stainless steel flange plates. To avoid deposition of vapors on the windows, water jacket was provided at the ends of each of the four arms. To start with, the heat pipe was thoroughly cleaned with hydrochloric acid and acetone. Clean stainless steel mesh was rolled into layers and was inserted in the arms of the heat pipe. The heat pipe was connected to the vacuum system through copper tubing. The vacuum system consisted of a rotary pump and an oil diffusion pump giving vacuum better than 10^{-4} torr. Gas filling arrangement consisted of a He cylinder and a glass bulb which served as a reservoir. The bulb was first evacuated and then filled in with He at about 520 torr pressure. Heat pipe was evacuated to a pressure less than 10^{-4} torr, and then filled with the He gas at the desired pressure. An oil manometer was used to monitor pressure. The central zone was heated using a heating tape wrapped uniformly around the heat pipe and a fire brick structure covered the heated zone to reduce convection losses. A chromel alumel thermocouple was used to monitor temperature of the central zone. A temperature controller (Aplab, Type PTC-372) was used to control the temperature to a desired value. The temperature variation was maintained within $\pm 5°C$. During this temperature variation the cadmium vapor pressure is nearly constant. The empty heat pipe (with mesh) was baked for several hours continuously at high temperature (about 500°C) under vacuum. Once the system was baked small pieces of pure cleaned cadmium metal were kept carefully at the center of the heat pipe. The system was then evacuated to $\leqslant 10^{-4}$ torr and then filled in with He gas at a desired pressure. The metal vapor plasma was generated by focussing Nd:YAG laser at the centre of the heat pipe. In order to study cadmium plasma in the presence of a high Z target, a tungsten target fixed to a rod was inserted into one of the arms of the heat pipe. The tungsten plasma was used as a pumping source to pump Cd vapors. To observe laser oscillations in Cd II at 441.6 nm a cavity was aligned normal to the direction of the incident (1.06 μm) laser beam. The pumping flux from the target is absorbed as it propagates through the vapor medium and hence affects the density and temperature of the vapor plasma. In order to account for the effect one needs to calculate plasma parameters viz. temperature and density.

2.1 *Temperature measurement*

The usually employed techniques to measure plasma temperature are a) Langmuir probes, b) measurement of intensity ratio of spectral lines. We have used line intensites of cadmium plasma to determine the electron temperature [26].

2.2 *Density measurement*

The electron density of a plasma is usually measured employing either the spectroscopic or an optical technique. In the former class the most widely used technique is to estimate Stark broadening of a particular transition [27]. For our present studies we have used optical technique to estimate density of the plasma. Optical diagnostics techniques are based on measuring the refractivity of a plasma by directly comparing the phase of a probe wavelength passing through the plasma with a reference. The measurement of phase shift provides us the density of electrons [28]. Studies on measurement of densities of electron and neutral atoms in a carbon plasma have been reported [29] using a two wavelength interferometry. In our studies we have used a Mach Zehnder interferometer [30] for measurement of plasma density. The experimental layout of Mach Zehnder interferometer is shown in figure 2. A $2\omega_0$ (0.532 μm) radiation was used as a probe beam. The collimated probe was split into two beams to equal intensity at beam splitter BS_1 and were recombined at the beam splitter BS_2. The dispersive element, plasma in a heat pipe oven in our case, is kept in one arm of the interferometer and a compensating glass plate is inserted in the

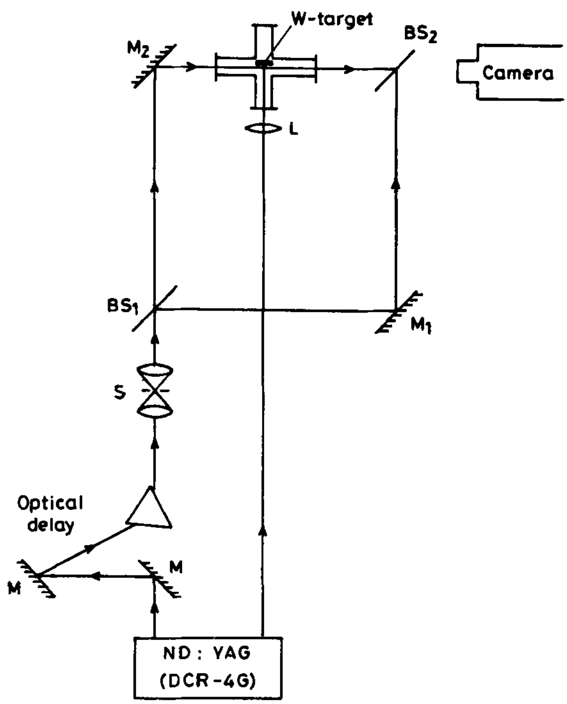

Figure 2. Mach Zehnder interferometer for density measurement.

other arm of the interferometer. The phase difference between the two beams is given by,

$$\Delta\varphi = \frac{2\pi}{\lambda_p}\int_0^{r_0}(1-\mu)\mathrm{d}y \tag{1}$$

where μ is the refractive index of the plasma, λ_p the probe wavelength, and r_0 is the size of the plasma. The phase difference $\Delta\varphi$ given by (1) produces a shift in the fringes. The interferograms thus obtained are analysed using Abel inversion technique [31]. The technique is used for finding the radial dependence of a quantity $\varepsilon(r)$ e.g. refractive index, emission coefficient etc. when measurements of the line integral of $\varepsilon(r)$ are made along the chords of an axially symmetric plasma or other dielectric medium. If the measured quantity is $N(x)$ for a chord distant x from the axis we have

$$N(x) = 2\int_0^{(r_0^2-x^2)^{1/2}}\varepsilon(r)\mathrm{d}y \tag{2}$$

$\varepsilon(r)$ is given by the Abel integral [31]

$$\varepsilon(r) = -\frac{1}{\pi}\int^{r_0}\frac{N'(x)}{(x^2-r^2)^{1/2}}\mathrm{d}x. \tag{3}$$

The integral (3) is evaluated numerically with $N'(x) = \partial N/\partial x$ being found [32] from the experimental data $N(x)$. Following Bockasten [31] the integral can be written as a series

$$\varepsilon_j = \frac{1}{r_0}\sum_{k=0}^{n-1} a_{jk}N_k \tag{4}$$

a_{jk}'s are the Abel coefficient, r_0 is the size of the plasma and N_k is the value of $N(x)$ for which $x = \{kr_0/n\}$, n is the number of channels. A computer programme was developed to calculate the Abel coefficients and also to calculate the radial dependence of electron density. From eqs (1), (2) and (4), we have

$$n_e(r) = \frac{4\pi^2 m\varepsilon_0 c^2}{e^2\lambda_p}\frac{1}{\Delta}\varepsilon_j \tag{5}$$

where Δ is the fringe spacing. Equation (5) gives the radial dependence of electron density.

Mach Zehnder interferometer has been used for measuring densities of various atomic and ionic levels in the laser excited barium vapor [33]. A 1 μs long dye laser pulse tuned at wavelength of 553.5 nm was used to excite Ba vapor. The probe beam used for interferometric studies was a 1 ns long broad band (417–608 nm) dye laser. Interferometric studies of laser induced surface heating and deformation of metal and semiconductor have also been carried out [34]. Time resolved electron density measurements in an ArF excimer laser discharge have been reported [28] using He–N_2 laser (337.1 nm) as a probe beam. Recently density measurement of Ti atoms, in laser produced Ti vapor plasma has also been reported [35]. The plasma was produced using a YAG laser of 1.5 ns duration, and a N_2 laser (337.1 nm) of 10 ns pulse duration was used as a probe beam. Other techniques like Schliren [36] and

Shadowgraphy [37] have also been employed for density measurement. These techniques depend on deviation of the beam which is proportional to the first and second derivatives of the electron density. In these techniques no separate reference beam is used; the intensity variations arise by virtue of local intensification of the probe beam due to refraction. Such systems are easy to align compared to interferometers but the analysis of the results is difficult.

3. Studies on cadmium metal vapor plasma

In this section studies on cadmium metal vapor plasma in the presence of a high Z LPP are presented. The laser beam from a Nd:YAG laser was focussed at the center of the heat pipe using a quartz lens. The temperature was slowly raised to 450°C with He gas pressure of 7 torr, no cadmium plasma was observed visually. However, when the buffer gas pressure was increased to 52 torr and the temperature kept at 400°C a weak cadmium plasma was observed. Increasing temperature further at the same buffer gas pressure increased the intensity of the plasma. An intense green ball of cadmium plasma could be seen on viewing through one of the side arms when the heat pipe was operated at 500°C. Figure 4 shows a Cd spectrum at temperature of 500°C and He pressure of 77 torr, recorded using a monochromator set up shown in figure 3. The laser energy was 900 mJ in 8 ns pulse. An estimate of the temperature of metal vapor plasma was made by taking ratio of the intensities of the spectral lines. The observed temperature is 0.5 eV. It was also observed that on increasing the temperature of the heat pipe beyond 500°C the intensity of the green blob decreased. This may be due to particulate formation [25, 38] the so-called 'fogging' in the heat pipe. To confirm and visually observe the formation of clusters, a weak He–Ne laser beam was sent close to the centre of the heat pipe. The pattern in transmitted laser beam was observed on a wall, about 4 m away from the heat pipe.

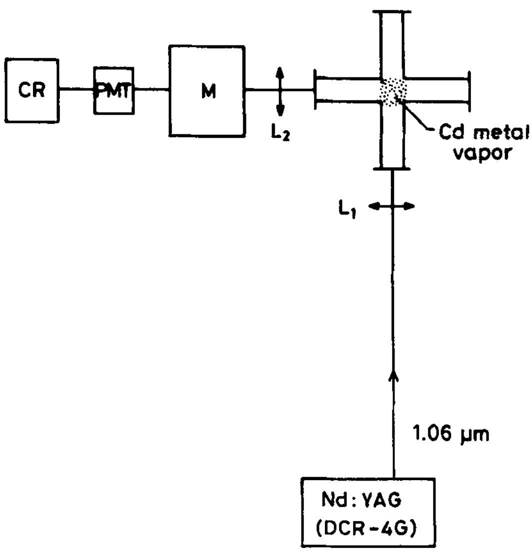

L_1, L_2 - Lenses ; M - Monochromator ; CR - Chart recorder ;
PMT - Photomultiplier tube

Figure 3. Experimental set-up for recording plasma emmision.

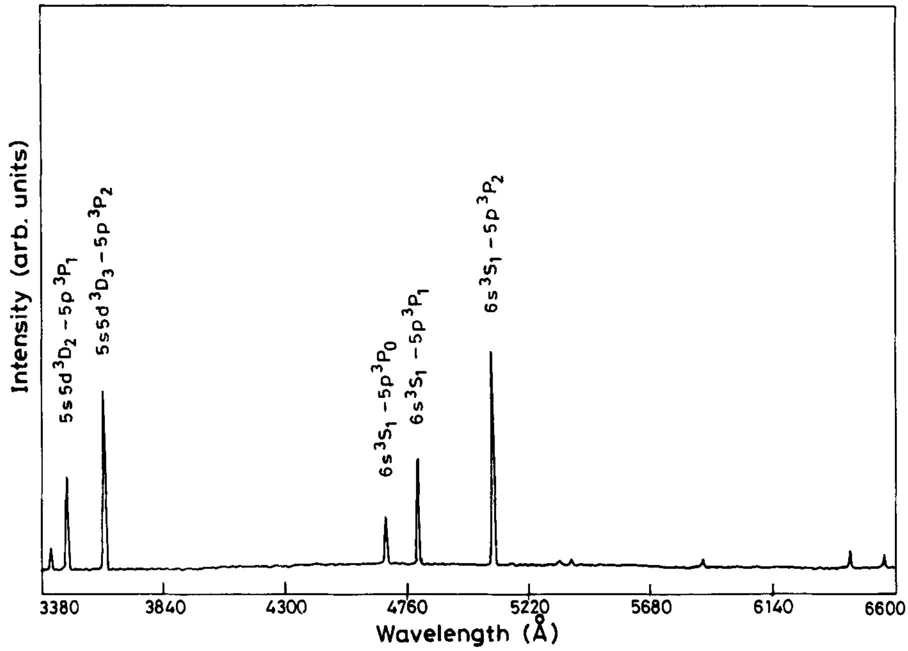

Figure 4. Visible spectrum of Cd metal vapor plasma at a He pressure of 77 torr.

The convective movement of the dust-like particles was clearly visible in the beam. We feel that this particulate formation is due to cadmium clusters created by condensation of the metal vapors in the cold zone at the boundary with the buffer gas. Similar effect was also observed if the central part of the heat pipe was suddenly overheated. Thus the poor conditions of operation for the heat pipe, result in cluster formation of the metal. Obtaining a high Cd density required for efficient plasma production appears to be the most difficult technical problem in the experiments, such as ours. Our experience shows that the temperature of the heat pipe should be increased very slowly and should not exceed the value at which the vapor pressure of the metal vapor and buffer gas pressure are equal [24].

In order to look at the possibility of using laser produced plasma as a pumping source for photo-ionization Cd^+ laser oscillating at 441.6 nm, a tungsten target fixed to a rod was inserted into one of the arms of the heat pipe opposite to the direction of the incident laser beam. The target rod was continuously rotated by an electric motor to avoid crater formation. The laser radiation was focussed to a spot of 100 μm onto the tungsten target with helium gas at a pressure of 7 torr. No heating of the heat pipe was done. A bluish white plasma of tungsten was visually seen at the target surface. The density of the laser produced tungsten plasma was estimated using a Mach Zehnder interferometer as described earlier in §2.2. Figure 5 shows the radial density distribution of tungsten plasma at a distance of 1–2 mm from the target. The delay between the 1.06 μm beam and the probe beam was 19 ns. This was the optimum value of the delay. For lower values the plasma expansion was very fast and the fringes close to the target were quickly merged, while for higher value of delays the shift was very small.

In order to photo-ionize the cadmium metal vapor, the heat pipe temperature was raised to 420°C with a He pressure of 7 torr and the laser radiation was focussed onto the tungsten target. We observe a bluish white plasma very close to the target

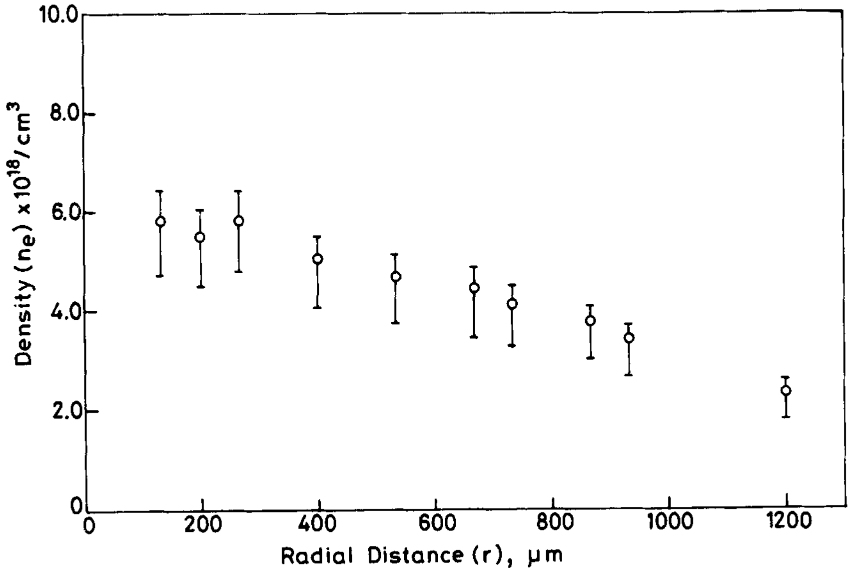

Figure 5. Radial density profile of tungsten plasma at 1–2 mm distance from the target.

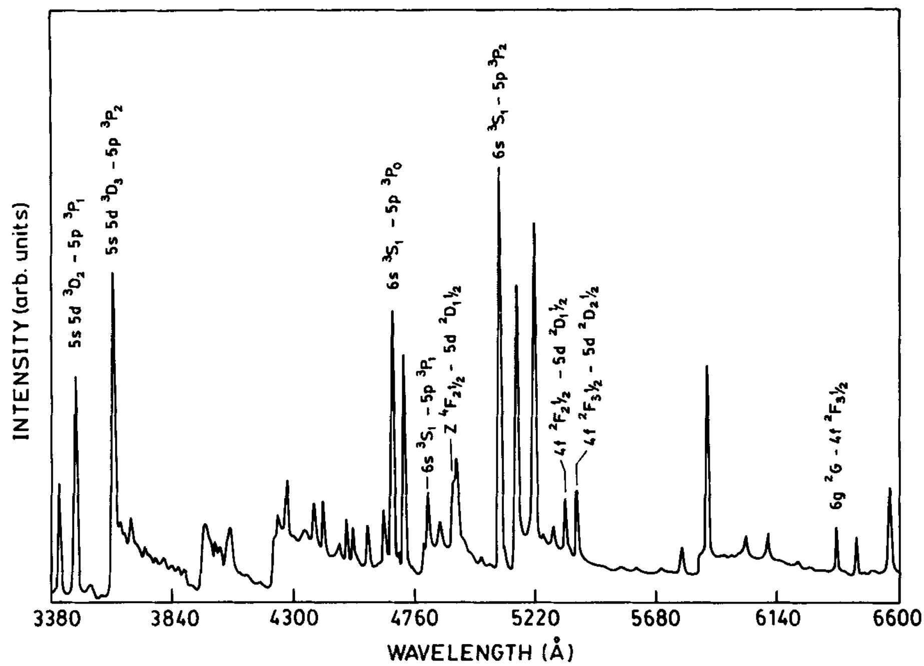

Figure 6. Visible spectrum of Cd metal vapor in the presence of tungsten plasma.

surface and green plasma due to cadmium vapor extending up to 8 mm away from the tungsten surface. The Cd emission spectrum shown in figure 6, recorded in the presence of tungsten target shows an increase in intensity of all lines and Cd II lines which were absent in figure 4 are also observed. Thus laser produced plasma can be a very effective source for getting higher ionic states. We estimate temperature of Cd plasma at 4 mm away from the surface of the target to be 0.3 eV.

4. Laser oscillations

Here we describe the laser oscillations on $4d^9 5s^2\ ^2D_{5/2} - 4d^{10} 5p\ ^2P_{3/2}$ transition at 441.6 nm using tungsten plasma as a pumping source. The population inversion occurs between the $4d^9 5s^2$ state and $4d^{10} 5p$ state. As said earlier, for high Z target continuum radiation dominates over the line radiation. The broad band soft X-ray emission from a laser produced plasma directly populates the upper laser level from the ground level. The pumping rate is essentially determined by the photon density of the pumping source. The fact that at short wavelength, inner-shell photo-ionization has a higher probability than ionization of a outer electron, the most probable process with the radiation peaked in the range 200–300 Å for high Z target is photo-ionization. The experimental set-up used by us for observing laser oscillations in Cd at 441.6 nm is shown in figure 7. A crossed heat pipe described in § 2 was used to produce homogeneous vapors of cadmium. The heat pipe was operated at 420°C with helium pressure of 7 torr. The cavity was formed using two He–Cd mirrors such that $g_1 g_2 \approx 0.65$. One of the mirrors was totally reflecting while the other had about 1% transmission at 441.6 nm, through which the laser output was monitored. The ends of the heat pipe along the axis of the resonator were fitted with windows set at Brewster angle. The optical axis of the resonator was parallel to the target (tungsten) surface. The output signal was sensitive to the alignment of the resonator axis, with a slight movement of either mirrors the stimulated emission fell to a very low value. The output was detected through a monochromator (HRS-2 Jobin-Yvon) using a photomultiplier tube (IP28, Hamamatsu, rise time 2.2 ns). To see the effect of the input laser energy (Nd:YAG) on the output of Cd II laser at 441.6 nm, experiment was performed at 100, 200 and 300 mJ of input energy. Figure 8 shows the variation of laser output with input laser (1.06 μm) energy. Because of target etching at high input energies we were not able to go beyond 300 mJ of input energy but it is expected that the laser output will increase with input energy. Although we observed laser oscillations close to the target surface, the optimum position of the resonator axis was found to be 4 mm away and parallel to the target surface. Since very close to the target surface the pumping flux is high, one expects high inversion densities but electron collisions depopulate the upper laser level. At larger distances the output is decreased due to the reduced pumping flux from the diverging X-rays. The coupling efficiency of the pumping flux and the lasing plasma depends on the configuration used for photo-ionizing source and metal vapor plasma. The emission from the laser

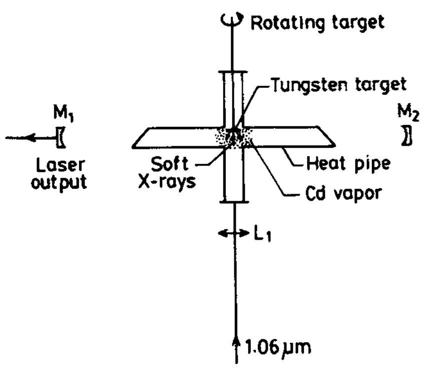

Figure 7. Experimental set-up for observing laser oscillations.

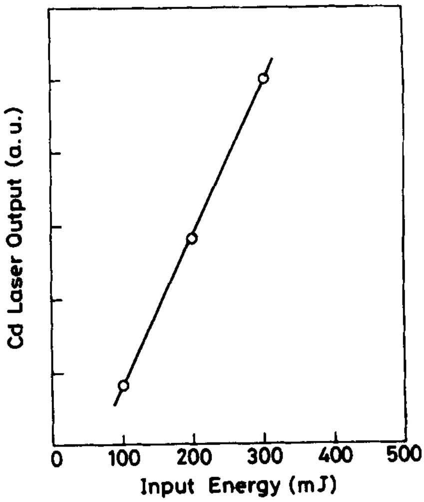

Figure 8. Variation of laser output with input laser (1·06 μm) energy.

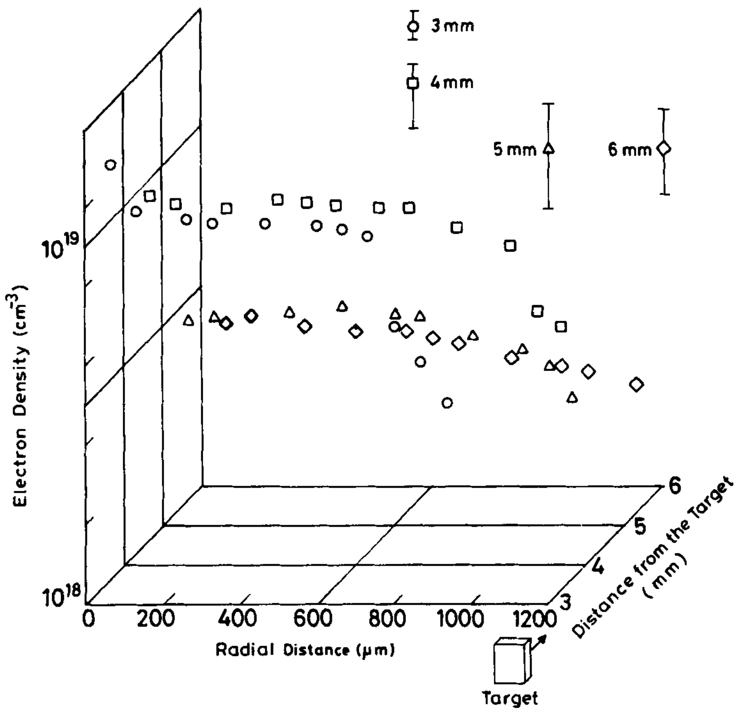

Figure 9. Radial density profiles of Cd plasma in the presence of tungsten target.

produced plasma source is absorbed as it propagates through the vapor medium and hence in our case affects the density and temperature of the medium. Thus the coupling between the background plasma and that of Cd plasma affects the pumping rate for a photo-ionization process. Figure 9 shows the radial profiles of electron density of cadmium plasma (in the presence of tungsten plasma) measured using the set-up shown in figure 2 at various distances from the target surface. The axial density can be obtained from the radial profiles and hence the effect of the density on the varying gain can be estimated. The high electron density observed close to the target surface shows the effect of plasma electrons. The influence of these electrons decreases as we move away from the target surface because for the given vapor pressure and within the excitation time these electrons penetrate only 2–3 mm into the vapor.

5.

Since our interest is in Cd II transitions, it is worthwhile to consider the possible routes for a Cd II transition at 441.6 nm (in particular). Although the process of inner-shell photo-ionization is dominant, one should also look at the effect of photoelectrons which are immediately present after photo-ionization. The energy distribution of the photoelectrons has a maxima around 40 eV and is determined by the photon energy distribution and wavelength dependence of the photo-ionization cross-section. If we compare the cross-sections [39, 40] for various levels of Cd we find that the cross-section for $5s^2$ levels are larger than $5p$ states in the region above 50 eV. Thus using a black body peaked in the range 200–300 Å one would expect that $5s^{2\,2}D$ states are formed almost exclusively by removal of innershell electron while the ordinary $5p$, $5d$, $6p$ states are formed by ionization of one electron and excitation of another electron.

Population inversion in photo-ionization lasers can be produced either by directly pumping the upper laser level or transferring population from a nearby directly pumped level to the upper laser level. It has been shown that the latter is less efficient possibly due to broadening of the laser transition during the transfer process [41]. Population inversion is also possible from states that are pumped by photo-ionization to lower lying bound or autoionizing states. The lower laser level being ground state of an ion. For such an inversion to occur the duration of the pumping source should be small so that efficient inversion is produced before electrons collide with neutral species and ionize them to produce ion ground state. The pumping rate depends on the density of photon from a laser produced plasma source interacting with metal vapor and $\sigma_{\rm pi}$ the photo-ionization cross-section to the upper laser level. The population of the upper level related to the ground state population can be written as

$$N_u = \frac{2W_p\sigma_{\rm pi}\exp(-\sigma_t Nr)\tau_P N}{h\nu_p\pi r^2}k_f \tag{6}$$

where W_p is the pumping power, N is the ground state population of the metal vapor and σ_t is the total absorption cross-section in the wavelength region that pumps the upper laser level. τ_P is the duration of the pumping X-ray pulse and is of same duration as that of the laser pulse used for creating soft X-rays, and k_f is the conversion efficiency of the incident flux into soft X-ray flux. It follows from (6) that for larger population of the upper state, the photon density N_ν should be large and the distance between active medium and the pumping source should be small. The gain length product GL can be written as

$$\mathrm{GL} \simeq N_u\sigma_{\rm se} L \tag{7}$$

where N_u is the population density of the upper level and, $\sigma_{\rm se}$ is the stimulated emission cross-section for the lasing wavelength (441.6 nm), L is the length of the gain medium. Using the values of various parameters and assuming $k_f \approx 1\%$, we get $\mathrm{GL} \sim 11$. The value of GL apart from other parameters depends on conversion efficiency k_f which depends on configuration, focussing condition, pulse width and wave-length of laser used for generation of photo-ionization source. The GL product can also be increased using a line pumping source. We have used single spherical plasma spot in our studies, however, using multifoci geometry to generate a multispot plasma one can increase total gain length.

In conclusion we studied the Cd metal vapor plasma in a crossed heat pipe. To study the effect of black body pumping, Cd metal plasma was studied in the presence of tungsten plasma. Laser oscillations were observed in Cd II on $4d^9 5s^2\ ^2D_{5/2} - 4d^{10} 5p\ ^2P_{3/2}$ transition at 441.6 nm using photo-ionization pumping scheme. The electron density was estimated using a Mach Zehnder interferometer.

Acknowledgement

This work is supported by the Department of Science and Technology, New Delhi.

References

[1] M A Duguay and P M Rentzepis, *Appl. Phys. Lett.* **10**, 350 (1967)
[2] S E Harris, J R Young, R W Falcone, J E Rothernberg, J R Willison and J C Wang in *Laser techniques for extreme ultraviolet spectroscopy*; edited by T J Mcllrath and R R Freeman (AIP, New York, 1982) p 147
[3] H W K Tom and O R Wood II, *Appl. Phys. Lett.* **54**, 517 (1989)
[4] W T Silfvast, J J Macklin and O R Wood II, *Opt. Lett.* **8**, 551 (1983)
[5] A J Mendelsohn and S E Harris, *Opt. Lett.* **10**, 128 (1985)
[6] W T Silfvast and O R Wood II, *J. Opt. Soc. Am.* **B4**, 609 (1987)
[7] H Lundberg, J J Macklin, W T Silfvast and O R Wood II, *Appl. Phys. Lett.* **45**, 335 (1984)
[8] M Hube, M Dieckmann, H Welling and B Wellegehausen, *J. Opt. Soc. Am.* **B6**, 1217 (1989)
[9] M Hube, R Brinkman, H Welling, R Beigang and B Wellegehausan, *Appl. Phys.* **B45**, 197 (1988)
[10] M Hube, J Michael and B Wellegehausen, *Opt. Lett.* **15**, 480 (1990)
[11] S J Benerofe, Yu Vin Guang, C P J Barty, J F Young, and S E Harris, *Phys. Rev. Lett.* **66**, 3136 (1991)
[12] M H Sher, J J Macklin, J F Young, and S E Harris, *Opt. Lett.* **12**, 891 (1987)
[13] H C Kapteyn and R W Falcone, *Phys. Rev.* **A37**, 2033 (1988)
[14] A M Weigold and J A Piper, *Opt. Lett.* **15**, 1209 (1990)
[15] O Sullivan, *J. Phys.* **B16**, 3291 (1983)
[16] T P Hughes, *Plasma and laser light* (Wiley, New York, 1975)
[17] J M Bridges, C L Cromer and T J Mcllrath, *Appl. Opt.* **25**, 2208 (1986)
[18] M D Rosen, D W Phillion, V C Rupert, W C Mead, W L Kruer, J J Thomson, H N Kornblum, V N Silvinsky, G J Caporaso, M J Boyle and K G Tirsell, *Phys. Fluids.* **22**, 2020 (1979)
[19] W R S Garton, K Codling, *Proc. Phys. Soc.* (*London*) **75**, 87 (1960)
[20] F S Tomkins and B Ercoli, *Appl. Opt.* **6**, 1299 (1967)
[21] G M Grover, T P Cotter and G F Erickson, *J. Appl. Phys.* **35**, 1990 (1964)
[22] C R Vidal, *J. Appl. Phys.* **44**, 2232 (1973)
[23] H Scheingraber and C R Vidal, *Rev. Sci. Instrum.* **52**, 1010 (1981)
[24] R Tambay, *Cadmium photo-ionization laser* Ph.D. Thesis, IIT Kanpur (1991)
[25] W Gawlik and R Neumann, *Opt. Commun.* **68**, 345 (1988)
[26] A Khare, V Kumar and R K Thareja, *Z Phys.* **D6**, 67 (1987)
[27] R Tambay, R Singh and R K Thareja, *J. Appl. Phys.* **72**, 1197 (1992)
[28] T Mochizuki, K Hirata, H Ninomiya, K Nakamura, K Maeda, S Horiguchi and Y Fujiwara, *Opt. Commun.* **72**, 30 (1989)
[29] C D David Jr, *Appl. Phys. Lett.* **11**, 394 (1967)

[30] W C Marlow, *Appl. Opt.* **6**, 1715 (1967)
[31] K Bockasten, *J. Opt. Soc. Am.* **51**, 943 (1961)
[32] R Illingworth and R K Thareja, *J. Phys.* **E14** 147 (1981)
[33] L Jahreiss and M C E Huber, *Phys. Rev.* **A28**, 3382 (1983)
[34] W K Lee and C C Davis, *IEEE J. Quantum Electron QE* **22** 3382 (1986)
[35] H Ninomiya, N Takashima and K Hirata, *J. Appl. Phys.* **69**, 67 (1991)
[36] T J Englert and M A Beik, *Rev. Sci. Instrum.* **61**, 3783 (1990)
[37] I H Hutchinson in *Principles of plasma diagnostics* (Cambridge University Press, 1987)
[38] M Allegrini, P Biechi, D Dattrino and L Moi, *Opt. Commun.* **49**, 39 (1984)
[39] T Goto, K Hane, M O Kuda and S Hattori, *Phys. Rev.* **A27**, 1844 (1983)
[40] W Lotz, *Z. Phys.* **220**, 466 1969
[41] W T Silfvast, O R Wood II, H Lundberg and J J Macklin, *Opt. Lett.* **10**, 122 (1985)